Article

Surface-Enhanced Raman Scattering and Polarized Photoluminescence from Catalytically Grown CdSe Nanobelts and Sheets

Rayapati Venugopal, Ping-I Lin, Chung-Chan Liu, and Yit-Tsong Chen

J. Am. Chem. Soc., **2005**, 127 (32), 11262-11268• DOI: 10.1021/ja044270j • Publication Date (Web): 20 July 2005

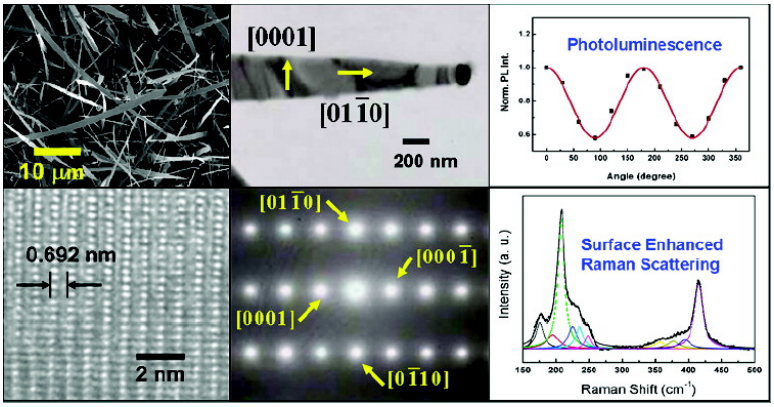

More About This Article

Additional resources and features associated with this article are available within the HTML version:

- Supporting Information
- Links to the 12 articles that cite this article, as of the time of this article download
- Access to high resolution figures
- Links to articles and content related to this article
- Copyright permission to reproduce figures and/or text from this article

View the Full Text HTML

J|A|C|S
ARTICLES
Published on Web 07/20/2005

Surface-Enhanced Raman Scattering and Polarized Photoluminescence from Catalytically Grown CdSe Nanobelts and Sheets

Rayapati Venugopal, Ping-I Lin, Chung-Chan Liu, and Yit-Tsong Chen*

Contribution from the Department of Chemistry, National Taiwan University, Taipei 106, Taiwan, and Institute of Atomic and Molecular Sciences, Academia Sinica, P.O. Box 23-166, Taipei 106, Taiwan

Received September 20, 2004; E-mail: ytchen@pub.iams.sinica.edu.tw

Abstract: We have successfully fabricated single-crystalline CdSe nanowires, nanobelts, and sheets by a chemical vapor deposition (CVD) method assisted with laser ablation. The synthesized CdSe nanostructures have hexagonal wurtzite phase as characterized by X-ray diffraction (XRD). CdSe nanobelts can range in length from several tens to a hundred micrometers, in thickness from 40 to 70 nm, and a tapered width which is ~3 μm at one end and tapers off to ~100 nm at a catalytic gold particle. Both selected area electron diffraction (SAED) and high-resolution transmission electron microscopic (HRTEM) measurements show that the single-crystalline hexagonal belts and sheets grew along the [0 1 −1 0] direction with side surface of ±(0 0 0 1) and top surface of ±(2 −1 −1 0). While the growth mechanism of nanobelts complies with a combination of vapor−liquid−solid (VLS) and vapor−solid (VS) processes, the formation of sheets is primarily based on the VS mechanism. For comparison, the phonon modes of CdSe nanobelts and bulk powder have been measured by surface-enhanced Raman scattering (SERS) and normal Raman scattering (NRS) spectroscopies with off- and near-resonant excitations. A blue-shift of 2.4 cm^{-1} for the longitudinal optical (LO) phonon of CdSe nanobelts, relative to bulk CdSe, is attributed to a lattice contraction in the belt structure, which is confirmed by the XRD measurement. Room-temperature microphotoluminescence (PL) at ~1.74 eV from single CdSe nanobelts shows a 3-fold enhancement compared to that from bulk CdSe powder and displays a partial polarization dependence of emission angles.

Introduction

Miniaturization of electronic devices at a nanoscale with appreciable optoelectronic enhancement in their high performance is as challenging as it is desirable in advanced material technology. Nanostructured materials have attracted a great deal of attention because of their novel physical, chemical, optical, mechanical, and optoelectronic properties.[1−3] In particular, CdSe nanocrystals have been proposed as the working elements for nanotransistors,[4] electrochromic materials,[5] and charge-coupling devices.[6] CdSe nanowires[7] and nanotubes[8] have also been fabricated using electrochemical and chemical methods and may find usages in fabricating optoelectronic devices, such as solar cells, where the power conversion efficiency of nanorods has been demonstrated to be higher than that of quantum dots.[9] Core−shell-structured CdSe/ZnS quantum dots exhibit a lasing effect and can be used for fluoro-immunoassays, biological imaging, and biosensors.[10]

Different from conventional nanowires, nanobelts can be nearly void of dislocations and line defects,[11] which substantially improve their electronic and optoelectronic performances. Among many recent applications of the belt-like nanostructures of semiconducting oxides,[12] gas sensors, for example, have been fabricated using single-crystalline SnO_2 nanobelts.[13] Taking advantage of the mechanical resonance behavior and bending modulus, uniformly structured ZnO nanobelts with rectangular cross-sections can be used as a nanocantilever or a nanoresonator in nanoelectromechanical systems (NEMS).[11,14] On the basis of their sensitive conductivities to environment, ZnO and SnO_2 nanobelts have been applied to build field effect transistors, which can be used as light and gas sensors.[15] Imaging, manipulating, and mechanical testing of the single nanobelts

(1) Cui, Y.; Lieber, C. M. *Science* **2001**, *291*, 851−853.
(2) Bachtold, A.; Hadley, P.; Nakanishi, T.; Dekker, C. *Science* **2001**, *294*, 1317−1320.
(3) Huang, Y.; Duan, X.; Cui, Y.; Lauhon, L. J.; Kim, K.; Lieber, C. M. *Science* **2001**, *294*, 1313−1317.
(4) Klein, D. L.; Roth, R.; Lim, A. K. L.; Alivisatos, A. P.; McEuen, P. *Nature* **1997**, *389*, 699−701.
(5) Wang, C.; Shim, M.; Guyott-Sionnest, P. *Science* **2001**, *291*, 2390−2392.
(6) Woo, W. K.; Shimizu, K. T.; Jarosz, M. V.; Neuhauser, R. G.; Leatherdale, C. A.; Rubner, M. A.; Bawendi, M. G. *Adv. Mater.* **2002**, *14*, 1068−1071.
(7) Xu, D.; Shi, X.; Guo, G.; Gui, L.; Tang, Y. *J. Phys. Chem. B* **2000**, *104*, 5061−5063.
(8) Jiang, X. C.; Mayers, B.; Herricks, T.; Nxia, Y. *Adv. Mater.* **2003**, *15*, 1740−1743.
(9) Huynh, W. U.; Dittmer, J. J.; Alivisatos, A. P. *Science* **2002**, *295*, 2425−2427.
(10) Goldman, E. R.; Balighian, E. D.; Mattoussi, H.; Kuno, M. K.; Mauro, J. M.; Tran, P. T.; Anderson, G. P. *J. Am. Chem. Soc.* **2002**, *124*, 6378−6382.
(11) Hughes, W. L.; Wang, Z. L. *Appl. Phys. Lett.* **2003**, *82*, 2886−2888.
(12) Pan, Z. W.; Dai, Z. R.; Wang, Z. L. *Science* **2001**, *291*, 1947−1949.
(13) Comini, E.; Faglia, G.; Sberveglien, G.; Pan, Z.; Wang, Z. L. *Appl. Phys. Lett.* **2002**, *81*, 1869−1871.
(14) Bai, X. D.; Gao, P. X.; Wang, Z. L.; Wang, E. G. *Appl. Phys. Lett.* **2003**, *82*, 4806−4808.
(15) Arnold, M. S.; Avouris, Ph.; Pan, Z. W.; Wang, Z. L. *J. Phys. Chem. B* **2003**, *107*, 659−663.

10.1021/ja044270j CCC: $30.25

of ZnO and SnO_2 have been exercised by Mao et al.[16] to demonstrate that such nanobelts can be used as a tip in atomic force microscopy.

In the study of growth mechanisms, CdSe nanosaws synthesized recently by Ma et al.[17] were proposed to be induced by a surface polarization to form the particular morphology. Dong et al.[18] have successfully fabricated CdS nanobelts and nanowires at distinctive growth conditions, in which high temperature favors the synthesis of nanobelts, while nanowires prefer to grow at lower temperature. Prompted by the foregoing, we report in this article a large-scale catalytic synthesis and spectroscopic characterizations of CdSe nanostructures (including belts, sheets, and wires, yet with a major focus on the CdSe belts) obtained by a chemical vapor deposition (CVD) method assisted with laser ablation.

Experimental Section

Catalytic Growth. Apparatus used for the CVD experiment is similar to that described in our earlier publication for the fabrication of silicon (Si) nanowires.[19] High-purity CdSe powder (Strem Chemicals, 99.999%) was used as source material for the growth of CdSe nanostructures. The CdSe powder was pressed into a pellet and placed inside a quartz tube in the middle of an electric furnace. Prior to synthetic reaction, the quartz tube was evacuated and heated to 825 °C. Meanwhile, an 8 nm thick gold (Au) film coated on a Si wafer (20 × 10 × 2 mm^3), used as a product collection substrate and located downstream to the carrier-gas flow at a position of 550 °C, was vacuum annealed to recrystallize into Au nanoparticles. A carrier-gas mixture of Ar (90%) and H_2 (10%) with a flow rate of 100 sccm was then introduced into the quartz tube until the pressure reaches 250 Torr. When the gas flow became steady, a pulsed Nd:YAG laser (Spectra Physics, GCR-190) with 1064 nm wavelength, 7 ns pulse duration, 30 Hz repetition rate, and ~15 mJ/pulse was ignited to ablate the CdSe target. The laser beam passing through a lens of 100 cm focal length was confined into 1.5 mm in diameter on the target sample. A computer-programmed control of the rotation and tilt of a mirror-mount has been designed to guide the laser beam moving from one spot on the target sample to another during the ablation process. As such, the aligned laser could ablate fresh sample-spots in the course of experiment. Furnace temperature was kept at 825 °C throughout the experiment. After reaction, large-scale dark-brown products were synthesized on a wide area of the Si substrate. Various morphological nanostructures were found to deposit at different collection positions, that is, at distinctive deposition temperature.

Electron Microscopic Characterizations. X-ray diffraction (XRD) spectra of the fabricated nanostructures were recorded using Scintag X1 diffractometer with Cu Kα ($\lambda = 1.5418$ Å) radiation at a scanning speed of 2°/min in 2θ ranging from 20 to 80°. The as-grown nanostructures were also characterized by scanning electron microscopy (SEM), energy dispersive spectrometry (EDS) (LEO 1530, field emission gun SEM + EDS), transmission electron microscopy (TEM), selected area electron diffraction (SAED), and high-resolution transmission electron microscopy (HRTEM) (JEOL JEM 2010 Analytical TEM at 200 and 400 kV).

Confocal Spectroscopic Measurements. Experimental details for the Raman and photoluminescence (PL) measurements of nanoscaled materials studied in this laboratory can be found in some earlier publications.[20−22] In the present study, Raman and PL investigations were performed in a confocal microscope (Jobin Yvon, 3143MFO) using an Ar−Kr ion laser (Coherent, Innova 70C) as an excitation light source (488 nm for Raman and 647 nm for PL), which was focused into a spot of ~4 μm in diameter on the samples. Both Raman and PL measurements were made in a 180° backscattering geometry. The Raman and PL signals were then sent into a monochromator (Jobin Yvon, Triax 550) equipped with a 1800 grooves/mm grating, and collected by a liquid-nitrogen-cooled charge-coupled device camera (Jobin Yvon, Spectrum-ONE; 1024 × 256 pixels). Near-resonance Raman scattering measurements with the 785 nm excitation of a diode laser were also carried out in a Nicolet Almega XR Dispersive Raman Spectrometer (Thermo Electron Corporation).

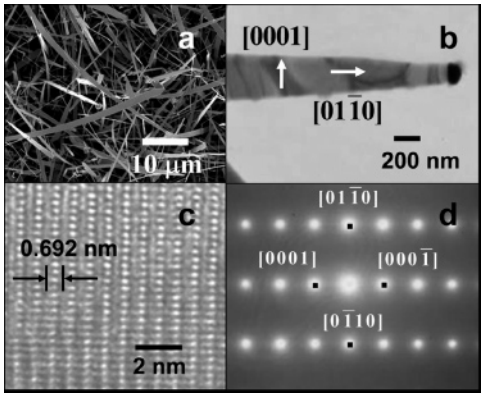

Figure 1. (a) SEM, (b) TEM, (c) HRTEM, and (d) SAED of as-synthesized CdSe nanobelts.

Observation of the phonon modes of single CdSe nanobelts has been made possible by surface-enhanced Raman scattering (SERS) spectroscopy with excitations at 488 nm (off-resonance) and 785 nm (near-resonance). In the SERS experiments, the CdSe nanobelts were dispersed freely on the surface of a 70 nm thick Au film coated on a Si wafer. The Au surface with roughness of ~6−10 nm in altitude, determined by an atomic force microscope (WITec, Alpha SNOM), was used to activate the surface-plasmon enhancement of Raman scattering signals. In the SERS measurements of CdSe nanobelts, care was taken to properly adjust the laser intensity of <9.32 kW/cm^2 to minimize a possible local heating and to avoid burning the nanobelts. To study both nanoscale and bulk structures, normal Raman scattering (NRS) spectrum of a pile of ca. five CdSe nanobelts on a Si wafer and the SERS and NRS spectra of bulk CdSe source powder have also been taken for comparison.

Room-temperature PL from single nanobelts was measured with 514 nm excitation at laser intensity of ≤0.7 kW/cm^2. To detect the PL from a single nanobelt, the excitation laser light was introduced into an objective lens (100X, NA = 0.9) of the confocal microscope. In an angle-resolved measurement for the PL polarization of single nanobelts at room temperature, the excitation laser at 647 nm was focused by an objective lens (50X, NA = 0.7) with laser intensity of ≤0.5 kW/cm^2.

Results and Discussion

Structural Determination and Growth Mechanism. The belts were generated with a high product yield at the deposition sites of 500−600 °C. Shown in Figure 1a is an SEM image of the CdSe nanobelts. Typical TEM image for a single CdSe belt of tapered width is depicted in Figure 1b, different from those nanobelts reported previously with either a uniform[12] or an

(16) Mao, S. X.; Zhao, M. *Appl. Phys. Lett.* **2003**, *83*, 993−995.
(17) Ma, C.; Ding, Y.; Moore, D.; Wang, X.; Wang, Z. L. *J. Am. Chem. Soc.* **2004**, *126*, 708−709.
(18) Dong, L.; Jiao, J.; Coulter, M.; Love, L. *Chem. Phys. Lett.* **2003**, *376*, 653−658.
(19) Yang, Y. H.; Wu, S. J.; Chiu, H. S.; Lin, P. I.; Chen, Y.-T. *J. Phys. Chem. B* **2004**, *108*, 846−852.
(20) Glinka, Y. D.; Lin, S. H.; Chen, Y.-T. *Phys. Rev. B* **2002**, *66*, 035404 and references therein.
(21) Miao, J.-Y.; Hwang, D. W.; Narasimhulu, K. V.; Lin, P.-I.; Chen, Y.-T.; Lin, S.-H.; Hwang, L.-P. *Carbon* **2004**, *42*, 813−822.
(22) Liu, Y.-C.; Lin, P.-I.; Chen, Y.-T.; Ger, M.-D.; Lan, K.-L.; Lin, C.-L. *J. Phys. Chem. B* **2004**, *108*, 14897−14900.

irregular shape in their widths.[18,23] Most of the belts can range in length from several tens to a hundred micrometers, thickness from 40 to 70 nm, and tapered width which is ~3 μm at one end and tapers off to ~100 nm at a catalytic particle. While surfaces of the fabricated CdSe belts in this work are clean without any amorphous sheath, the bending contours (Figure 1b) have been caused by bending-induced strain.[24] An EDS analysis reveals that the belts are composed of Cd and Se with a stoichiometric ratio close to 1:1, without contamination from the Au catalyst. Comparatively, a tip at the front-end of the nanobelt (Figure 1b) comprises major Au and minor Cd and Se. Panels c and d of Figure 1 depict the HRTEM image and SAED pattern of a CdSe nanobelt, respectively. The HRTEM image demonstrates clearly a single-crystalline structure with 0.692 ± 0.005 nm lattice spacing, corresponding to the (001) interplanar distance of hexagonal CdSe. The SAED pattern further reveals a hexagonal wurtzite structure of $a = 4.287$ Å and $c = 6.924$ Å for the CdSe nanobelt. As shown in Figure 1b, the CdSe nanobelts grew along the [0 1 −1 0] direction with side surfaces of ±(0 0 0 1) and top surfaces of ±(2 −1 −1 0). In the formation of CdSe nanobelts, we have observed that the fastest and relatively slower growth rates are along the [0 1 −1 0] and ±[0 0 0 1] directions, respectively, corresponding to the length (*b*-axis) and width (*c*-axis) of a belt, similar to those observed in CdSe nanosaws.[17]

In the XRD pattern of as-synthesized CdSe nanobelts (see Supporting Information Figure S1), prominent (100), (002), and (101) planes in a hexagonal wurtzite crystallite are identified, respectively, at 2θ of 24.024, 25.552, and 27.262, which compare with 23.928, 25.455, and 27.162 for the CdSe source powder (Supporting Information Figure S2). All XRD peaks of the CdSe nanobelts can be assigned to a hexagonal structure with lattice constants of $a = 4.277$ Å and $c = 6.971$ Å, in comparison with $a = 4.293$ Å and $c = 6.998$ Å of the CdSe source powder. Taking the angular resolution of $2\theta = 0.03°$ in the XRD instrument into account, lattice contractions of $a = 0.37 \pm 0.14\%$ and $c = 0.38 \pm 0.14\%$ in the CdSe belts have been determined from the XRD peak-shifts relative to bulk CdSe. The lattice contractions could have been induced by a surface tension during surface reconstruction in the growth of nanocrystallites.[25] In the fabrication of nanobelts in this work, CdSe vapor kept on depositing to the surface of the already formed nanobelts (a vapor−solid mechanism, and will be discussed later) which could have caused the surface reconstruction of nanobelts during the growing process. Similar lattice-contraction effect was also reported to exist in the growths of free-standing CdSe nanocrystals,[25] $CdS_{1-x}Se_x$ nanocrystals in glass matrices,[26] and CdSe quantum dots in glass matrices.[27]

In the XRD measurements of CdSe nanobelts, no other crystalline impurities were detected within the detection limit, except that a peak originates from the Si substrate (Supporting Information Figure S1). Sharpness of the XRD peaks indicates that the products are highly crystalline. It is well-known that a narrower XRD peak corresponds to a wider crystalline range

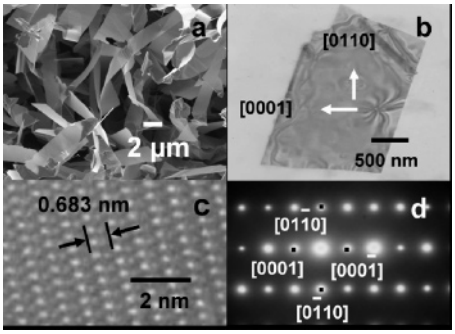

Figure 2. (a) SEM, (b) TEM, (c) HRTEM, and (d) SAED of as-synthesized CdSe sheets.

and/or lesser residual microstrain. The crystalline range of CdSe nanobelts, estimated from the widths of the (100) and (101) XRD peaks using Scherrer equation, gives 911 ± 15 and 977 ± 15 Å, respectively, in comparison with the crystallite sizes of 618 ± 15 and 540 ± 15 Å for the CdSe source powder in the same measurements. The obtained XRD data indicate that the as-grown CdSe nanobelts have a single phase of hexagonal wurtzite structure, in good agreement with the HRTEM and SAED results discussed earlier.

In this experiment, abundant CdSe nanowires have also been formed at 250−350 °C deposition sites (not shown). The fabricated CdSe nanowires have diameters ranging from 80 to 150 nm and can be a few hundreds of micrometers long. XRD data show that the as-synthesized CdSe nanowires have a hexagonal structure, as well. In the 650−700 °C deposition region, the synthesized CdSe structures were found to have sheetlike morphology (Figure 2) and will be discussed later. From our experimental results, it becomes clear that while higher deposition temperature favors the fabrications of belts and sheets, nanowires prefer to grow at a relatively lower temperature. This outcome is consistent with the formations of nanobelts and nanowires of CdS[18] and ZnO[23] reported earlier. In this experiment, morphologies of the CdSe nanostructures could be selected by adjusting the deposition positions at different thermal conditions. In addition, the widths and lengths of as-synthesized belts and sheets are quite sensitive to the reaction time and temperature. No obvious changes in the widths and lengths of the CdSe nanostructures, however, have been found by varying the flow rate of carrier-gas (Ar + H_2) at 100−200 sccm, or the ratio of H_2 in the Ar + H_2 mixture from 10 to 20%.

SEM image in Figure 2a shows a large quantity of sheetlike structures of several tens of micrometers length, 2−5 μm width, and ~40−50 nm thickness. The as-synthesized sheets are morphologically different from previously reported CdO sheets of rectangle, triangle, or parallelogram shapes.[11] XRD pattern of the as-synthesized sheets is similar to that of the CdSe nanobelts, with the peak positions being almost the same, except with a little difference in intensity ratio. A hexagonal wurtzite structure of the CdSe sheets with $a = 4.277$ Å and $c = 6.991$ Å has been determined from the XRD analysis, also indicating a lattice contraction in the CdSe sheets relative to bulk material. Typical TEM image of a single CdSe sheet is displayed in Figure 2b. EDS analysis for this sheet gives a stoichiometric ratio of Cd:Se close to 1:1. The CdSe sheet grows along the [0 1 −1 0] direction with side surfaces of ±(0 0 0 1) and top surfaces of ±(2−1−1 0), the same as those of CdSe belts.

(23) Yao, B. D.; Chan, Y. F.; Wang, N. *Appl. Phys. Lett.* **2002**, *81*, 757−759.
(24) Wang, Z. L.; Kang, Z. C. *Functional and Smart Materials: Structure Evolution and Structure Analysis*, Plenum: New York, 1998.
(25) Zhang, Z. Y.; Yong, X. Y.; Xiao, M. *Appl. Phys. Lett.* **2002**, *81*, 2076−2078.
(26) Scamarcio, G.; Lugara, M.; Manno, D. *Phys. Rev. B* **1992**, *45*, 13792−13795.
(27) Hwang, Y.-N.; Shin, S.; Park, H. L.; Park, S.-H.; Kim, U.; Jeong, H. S.; Shin, E.; Kim, D. *Phys. Rev. B* **1996**, *54*, 15120−15124.

HRTEM and SAED (c and d of Figure 2) of the CdSe sheet further confirm its single-crystalline interplanar distance of $d_{(001)} = 0.683 \pm 0.005$ nm and hexagonal wurtzite structure of $a = 4.266$ Å and $c = 6.928$ Å.

Our investigation at several experimental conditions shows that catalytic Au nanoparticles initiated the growth of CdSe nanowires and nanobelts. For the formation of CdSe nanowires, CdSe vapor was carried by Ar + H_2 and deposited onto liquid Au nanoparticles in the initial stage. When the dissolution of CdSe in the Au particles became supersaturated, CdSe nanowires extruded from the liquid Au catalysts and precipitated at the liquid−solid interface. This process basically complies with an ordinary vapor−liquid−solid (VLS) growth model proposed originally by Wagner et al.,[19,28] in which a liquid cluster of metal−catalyst provides energetically favored sites for the absorption/adsorption of gas-phase reactants. Sizes of the catalysts are considered to be responsible for the resultant diameters of nanowires. In our experiment, the fabrication of the CdSe nanowires at 250−350 °C is regarded to follow this VLS mechanism, where diameters of the nanowires are basically governed by the sizes of catalytic Au particles.

However, this VLS mechanism alone is inadequate to explain the growth of CdSe nanobelts, whose tapered widths increase gradually along the growth axis starting from the contact region between liquid Au nanoparticle and solid CdSe nanostructures. There should be some additional processes and crystallization kinetics that are more appropriate to describe the formation of the tapered CdSe nanobelts. Among other possibilities, subsequent deposition of CdSe vapor directly onto the already VLS-formed CdSe nanowires, known as a vapor−solid (VS) process,[29] can nicely account for the formation of the tapered CdSe nanobelts. This growth mechanism of the CdSe belts is analogous to that of CdS belts proposed by Dong et al.[18] In general, it requires more thermal energy to promote a VS growth than a VLS process.[12] Accordingly, more sample vapor is available in this higher-temperature region to initiate the VS growth. In this experiment, the CdSe nanobelts were fabricated at a higher-temperature deposition site (500−600 °C) than were the VLS-based CdSe nanowires (250−350 °C), thus supporting the proposed VLS + VS mechanisms for the formation of tapered structures. In contrast, the growth of CdSe sheets is considered to be governed mainly by a VS mechanism and requires a further study in the future. In view of the fact that the sheets grew at a deposition site of >650 °C, a VS process should dominate over the VLS growth in this high-temperature region.

Surface-Enhanced Raman Scattering (SERS). In the study of phonon modes of single CdSe nanobelts, we have conducted the vibrational measurements by surface-enhanced Raman scattering (SERS) and normal Raman scattering (NRS) spectroscopies. To assist spectroscopic assignment, the Raman experiments were performed with both off-resonant excitation at 488 nm (≈2.54 eV, above the band gap of ∼1.74 eV for CdSe) and near-resonant excitation at 785 nm (≈1.58 eV). Raman shifts in bulk CdSe source powder have also been measured in comparison with those of CdSe nanobelts.

Graphs a and b of Figure 3 show the SERS spectra of single CdSe nanobelts, with (a) off-resonance at 488 nm and (b) near-resonance at 785 nm excitations, which were taken from the same spot of a nanobelt lying on an Au film coated on a Si wafer. While the laser intensity was kept at 9.32 kW/cm^2 for the two excitations, signals in the off-resonant excitation (Figure 3a) are much weaker than those at near-resonance (Figure 3b). Although the integration time for signal acquisition was set 8 times longer in the off-resonance measurement, the signal-to-noise (S/N) ratio due to resonance enhancement is still better by a factor more than 20, as can be compared in a and b of Figure 3. These distinctive S/N ratios have demonstrated an enhancement effect of resonant excitation.

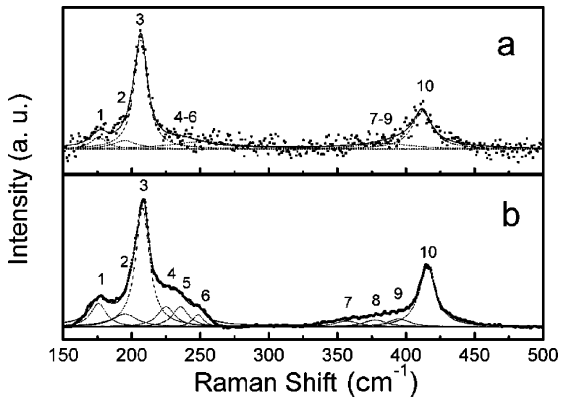

Figure 3. SERS spectra of a single CdSe nanobelt with excitations at (a) 488 nm and (b) 785 nm. While dots in the graphs represent raw spectral data, solid lines illustrate the fitted spectra. Deconvoluted phonon modes (dotted bands) are labeled and assigned. 1, TO (175.8 cm^{-1}); 2, SO (195.0 cm^{-1}); 3, LO (207.9 cm^{-1}); 4, LO + TA (225.1 cm^{-1}); 5, LO + LA (235.6 cm^{-1}); 6, LO + Γ_6 (248.4 cm^{-1}); 7, 2TO (356.8 cm^{-1}); 8, TO + LO (377.4 cm^{-1}); 9, SO + LO (395.0 cm^{-1}); 10, 2LO (415.6 cm^{-1}).

It is noteworthy that in an attempt to obtain the NRS spectrum of single CdSe nanobelts with 488 nm excitation, no NRS signal was able to be detected (before burning the belts) even under high laser power excitation. In contrast, the SERS signals of a single CdSe nanobelt could be detected with 488 nm excitation (Figure 3a), indicating an enhancement effect by Au surface plasmons. Raman shifts of a CdSe nanobelt, as marked by the deconvoluted bands 1−10 in Figure 3, have been observed at (1) 175.8 cm^{-1}, (2) 195.0 cm^{-1}, (3) 207.9 cm^{-1}, (4) 225.1 cm^{-1}, (5) 235.6 cm^{-1}, (6) 248.4 cm^{-1}, (7) 356.8 cm^{-1}, (8) 377.4 cm^{-1}, (9) 395.0 cm^{-1}, and (10) 415.6 cm^{-1}.

According to many previous studies,[30−32] the prominent Raman peaks of 1 (175.8 cm^{-1}), 3 (207.9 cm^{-1}), and 10 (415.6 cm^{-1}) in Figure 3 can be readily identified as transverse optical (TO), longitudinal optical (LO), and 2LO phonons, respectively. In an early study of Raman shifts in bulk CdSe single crystals, Yu[33] identified the phonon modes of LO + TA (transverse acoustic) at 219 cm^{-1}, LO + LA (longitudinal acoustic) at 229 cm^{-1}, and LO + Γ_6 ($\omega_{\Gamma_6} \sim 35$ cm^{-1}) at 247 cm^{-1}, where the relaxation of photoexcited B excitons to the A excitons of CdSe by acoustic phonons (TA and LA) via piezoelectric exciton−phonon interaction was employed to explain the vibrational observations.[33,34] Although the excitation wavelengths (785 and 488 nm) in the present experiment of CdSe nanobelts are

(28) Wagner, R. S.; Ellis, W. C. *Appl. Phys. Lett.* **1964**, *4*, 89−90.
(29) Brenner, S. S.; Sears, G. W. *Acta Mater.* **1956**, *4*, 268−270.
(30) Plotnichenko, V. G.; Mityagin, Y. A.; Vodop'yanov, L. K. *Sov. Phys. Solid State* **1977**, *19*, 1584−1586.
(31) Beserman, R. *Solid State Commun.* **1977**, *23*, 323−327.
(32) Arora, A. K.; Ramdas, A. K. *Phys. Rev. B* **1987**, *35*, 4345−4350.
(33) Yu, P. Y. *Solid State Commun.* **1976**, *19*, 1087−1090.
(34) Yu, P. Y. In *Excitons*; Cho, K., Ed.; Springer: Berlin, 1979; Chapter 15, pp 211−253.

different from the previous one (671 nm) by Yu[33,34] and the relaxation mechanisms require a further study in the future,[35−38] we have assigned the deconvoluted bands of 4 (225.1 cm^{-1}), 5 (235.6 cm^{-1}), and 6 (248.4 cm^{-1}) in Figure 3 as LO + TA, LO + LA, and LO + Γ_6, respectively, based on the similar phonon frequencies in both observations. It is also noted that these bands are much more enhanced with laser excitation at 785 nm (Figure 3b) than at 488 nm (Figure 3a).

A surface optical (SO) phonon with its frequency between those of TO and LO modes has been reported in the NRS observations of CdSe nanospheres[39] and CdSe quantum dots in glass matrix,[40] where the SO mode was induced by the chemical connection between a dielectric substrate and the nanocrystallites of interest. Furthermore, an electron−phonon coupling of Fröhlich interaction in CdSe nanocrystals relating to the LO and weak SO phonons has been investigated.[39,41] In this study, a deconvoluted weak signal at 195.0 cm^{-1} (peak 2 in Figure 3) has been assigned to the SO mode. In Figure 3b, other deconvoluted bands of 7 (356.7 cm^{-1}), 8 (377.4 cm^{-1}), and 9 (395.0 cm^{-1}) in the lower frequency wing of the 2LO band (415.6 cm^{-1}) have been assigned to 2TO, TO + LO, and SO + LO, respectively. Parts of these overtones and combination bands were also observed in the CdSe nanospheres.[39] In this study, laser power dependence of the SERS intensity for the observed phonon modes of CdSe nanobelts with excitation at 785 nm has also been investigated (Supporting Information S4).

Graphs a and b of Figure 4 show the SERS (solid line) and NRS (dashed line) spectra of CdSe in the structures of (a) source powder and (b) nanobelts. All of the spectra were measured with 785 nm excitation at laser intensity of 9.32 kW/cm^2. For comparison, the spectra of SERS and NRS were both normalized to the intensity of the LO band, although the intensity of SERS is generally much stronger than that of NRS. Taking a close look at the difference between SERS and NRS signals, represented by the underneath dotted lines in a and b of Figure 4, several phonon modes have been enhanced in the SERS measurement, among which the SO mode (peak 2) was magnified sizably by Au surface plasmons. The prime magnification of SO phonons in the SERS experiment can be rationalized by the fact that SO phonons execute vibrational motions only within a few atomic layers near the surface,[42] and the Raman scattering volume of this SO mode can entirely be subjected to the electromagnetic interaction with the Au surface

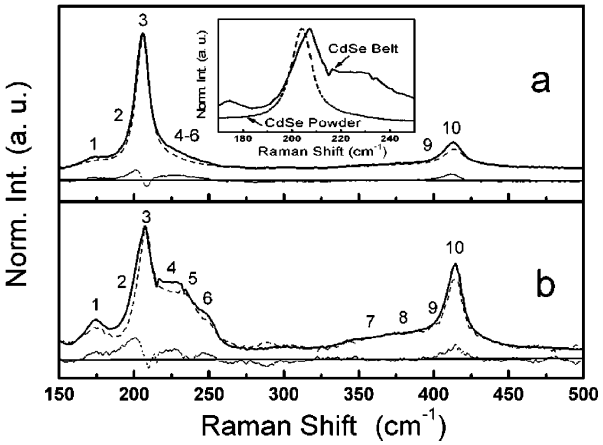

Figure 4. SERS (solid trace) and NRS (dashed trace) spectra of CdSe in the structures of (a) source powder and (b) nanobelts. All of the spectra were measured with 785 nm excitation at laser intensity of 9.32 kW/cm^2. For comparison, the spectra have been normalized to the intensity of LO mode. Dotted lines underneath represent the subtraction of NRS from SERS. Inset shows a spectral shift of 2.4 cm^{-1} for the LO modes in nanobelts (solid peak) and source powder (dotted peak).

plasmons. It is also noted that the surface-related phonon modes, such as SO and SO + LO (peak 9), have been more enhanced in the nanobelt (Figure 4b) than in the source powder (Figure 4a), which can be attributed to the high surface-to-volume ratio in nanobelts and a wide contact area between the belts and Au surface.

In Figure 4, more phonon modes of CdSe have been activated in the nanobelts (Figure 4b) compared to the two prominent LO and 2LO modes observed in the source powder (Figure 4a). Although CdSe nanobelts and source powder are both of hexagonal wurtzite crystalline structures, better crystallinity in the nanobelts could have allowed lattices to vibrate more collectively and phonons to propagate in a wider range, thus enhancing the Raman scattering volumes of the observed phonon modes.

In the present study, SERS spectra of single CdSe nanobelts enhanced by Cu and Ag substrates have also been observed (not shown), in which all the modes appear at the same peak positions as those enhanced by the Au surface. Suh and Lee[43] reported that the SERS signals of CdS nanowires, which grew epitaxially on the silver surface in the pores of anodic aluminum oxide, are enhanced by a local electric field near the Au surface rather than by a chemical effect. Theoretical and experimental studies of SERS mechanisms in many cases also indicate that SERS signals are mainly enhanced by the electromagnetic excitation of strongly localized surface plasmons.[44] In our observed SERS spectra, we also count the electromagnetic effect mostly responsible for the enhancement of Raman scattering. Chemical effect is less likely because there is no obvious charge transfer between the metallic Au surface and the semiconducting CdSe, which would have caused peak shifts between the SERS and NRS spectra (Figure 4a,b).

In the measurements of Raman shifts, the LO mode appears at 205.5 cm^{-1} for CdSe source powder (Figure 4a) and shows up at 207.9 cm^{-1} for CdSe nanobelts (Figure 4b). The LO phonon in CdSe was reported to vibrate along the *c*-axis.[27] The blue-shift of LO mode by 2.4 cm^{-1} in the CdSe nanobelts (inset

(35) In the present experiment, the excitation of CdSe nanobelts at 785 nm (≈1.58 eV) is still short of energy to create A excitons (∼1.74 eV) in CdSe crystals. Nevertheless, an intermediate state at ∼1.4−1.7 eV associated with Se vacancies in CdSe crystals has been reported in refs 36−38. In Supporting Information S3, we present the SERS spectra of single CdSe nanobelts excited at 785 nm with laser polarizations both parallel ($||_c$) and perpendicular ($\perp_c$) to the *c*-axis of CdSe nanobelt. In the $||_c$ excitation, a weak broad emission band at ∼1.43 eV was observed (Figure S3a), while with $\perp_c$ excitation, this emission band disappeared (Figure S3b). This observation suggests the existence of an intermediate state at ∼1.43 eV in CdSe nanobelts. In the present Raman experiment of CdSe nanobelts with 785 nm (≈1.58 eV) excitation, this state of ∼1.43 eV could also serve as an intermediate, besides the A exciton at ∼1.74 eV, for near-resonant Raman scattering.

(36) Rai, B. K.; Bist, H. D.; Katiyar, R. S.; Nair, M. T. S.; Nair, P. K.; Mannivannan, A. *J. Appl. Phys.* **1997**, *82*, 1310−1319.
(37) Garcia-Jimenez, J. M.; Martinez-Montes, G.; Silva-Gonzalez, R. *J. Electrochem. Soc.* **1992**, *139*, 2048−2052.
(38) Jager-Waldau, R.; Stucheli, N.; Braun, M.; Lux-Steiner, M.; Bucher, E.; Tenne, R.; Flaisher, H.; Kerfin, W.; Braun, R.; Koschel, W. *J. Appl. Phys.* **1988**, *64*, 2601−2606.
(39) Klein, M. C.; Hache, F.; Ricard, D.; Flytzanis, C. *Phys. Rev. B* **1990**, *42*, 11123−11132.
(40) Hwang, Y.-N.; Park, S.-H.; Kim, D. *Phys. Rev. B* **1999**, *59*, 7285−7288.
(41) Ruppin, R. *J. Phys. C* **1975**, *8*, 1969−1978.
(42) Esser, N. *Appl. Phys. A* **1999**, *69*, 507−518.
(43) Suh, J. S.; Lee, J. S. *Chem. Phys. Lett.* **1997**, *281*, 384−388.
(44) Tian, Z. Q.; Ren, B.; Wu, D. Y. *J. Phys. Chem. B* **2002**, *106*, 9463−9483.

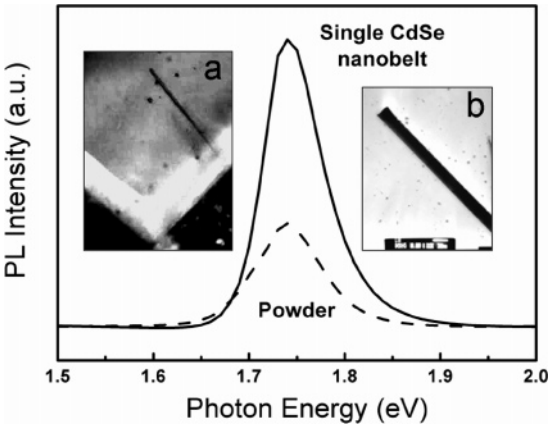

Figure 5. Micro-PL spectra of a single CdSe nanobelt (solid line) and bulk CdSe source powder (dashed line) excited at 514.5 nm with a laser intensity of 0.7 kW/cm^2. (a) Confocal microscopic image of a single CdSe nanobelt dispersed on a TEM grid. (b) TEM image of the same CdSe nanobelt in (a).

of Figure 4), relative to the bulk CdSe source powder, is due to a lattice contraction in the nanobelts which can be represented as[26]

$$\Delta\omega = \omega_{\mathrm{L}}\left[\left(1 + \frac{3\Delta c}{c}\right)^{-\gamma} - 1\right] \qquad (1)$$

where $\Delta\omega$ is the phonon frequency shift, $\gamma = 1.1$ is the Gruneisen parameter for CdSe,[45] ω_{L} is the LO frequency of bulk CdSe, and $\Delta c/c$ is the lattice contraction along the *c*-axis. On the basis of the observed blue-shift of 2.4 cm^{-1}, lattice contraction of $\Delta c/c \sim 0.35\%$ is calculated from eq 1, which is consistent with $\Delta c/c = 0.38 \pm 0.14\%$ determined from the XRD measurement as discussed earlier. In previous XRD and Raman studies, Zhang et al.[25] reported a similar lattice contraction of $\Delta c/c = 0.06$ and 0.23% for free-standing CdSe quantum dots of 5.6 and 3.9 nm diameter, respectively. In the Raman spectra of $CdS_{1-x}Se_x$ nanocrystals, prominent size dependencies (~5−20 nm in diameter) on a blue-shift caused by lattice contraction and on a red-shift due to quantum confinement have also been examined,[26] where the blue-shift dominates. In our study, since the scales of all dimensions (thickness, width, and length) in the CdSe nanobelts exceed ~40 nm, quantum confinement on the phonon motions due to the size effect is unlikely to make a significant contribution to the spectral shift. This also supports that the observed blue-shift of Raman scattering in the CdSe nanobelts originates from the lattice contraction.

Photoluminescence Polarization. Observed microphotoluminescence (PL) of the as-grown CdSe nanobelts is so strong that the detection of PL from a single nanobelt has been made possible. Figure 5 displays the micro-PL spectrum of a single CdSe nanobelt (solid line) in comparison with that of CdSe powder (dashed line) examined in the same experimental condition. A strong emission band at ~1.74 eV is observed, which corresponds to the energy band gap (E_{g}) of the CdSe nanobelt. For the PL spectrum of a single CdSe sheet in the same measurement (not shown), there is no significant difference from that of the CdSe nanobelt. It is noteworthy that the PL band of the CdSe nanobelt is 3-fold stronger than that of CdSe powder, as shown in Figure 5. The stronger PL intensity from

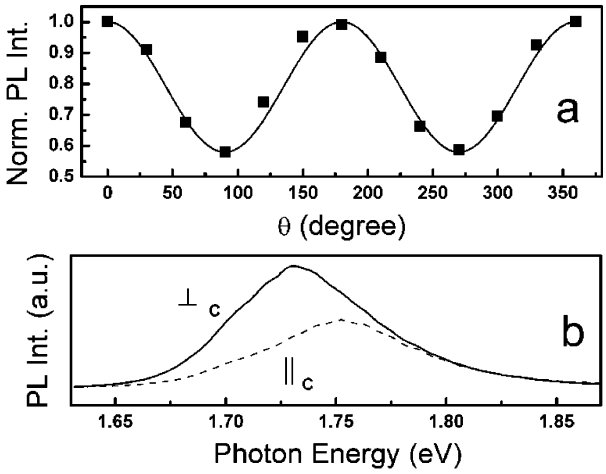

Figure 6. PL polarization of a single CdSe nanobelt excited at 647 nm with a laser intensity of 0.5 kW/cm^2. (a) Normalized PL intensities as a function of emission angles. The solid line represents a fit of $\cos^2\theta$. (b) Micro-PL spectra detected with the emission polarizations $\perp_c$ (solid line) and $||_c$ (dashed line) to the *c*-axis of the CdSe nanobelt, corresponding to the maxima and minima of PL intensities in (a), respectively.

the CdSe nanobelt can be attributed to both high crystallinity,[46] in accordance with the XRD result discussed earlier, and well synthesized surface of a nanocrystalline, which effectively prevents the CdSe nanobelts from carrier-quenching defects and nonradiative traps.[25] As-synthesized CdSe nanobelts and sheets are also stable upon aging for several months, demonstrated by a PL examination. In Figure 5, while a symmetric PL band-shape was observed for bulk CdSe powder caused by crystal imperfection and dislocations resulting in band-tail state transitions in the lower energy end, a little asymmetric PL band-shape with a steeper shoulder at the low-energy side is found for the nanobelt, which provides another evidence for the well crystallized CdSe nanobelts.[47]

Figure 6a shows the polarized micro-PL intensity of a single CdSe nanobelt as a function of emission angles. A laser at 647 nm with linear polarization parallel to the *b*-axis (length) of the belt was used as an excitation source. Maximum PL from the belt was detected when the polarizations of emission and excitation became parallel. The observed PL intensity oscillates as a function of $\cos^2\theta$ (θ is the angle between the polarizations of emission and excitation), rendering a degree of polarization, $(I_{\max} - I_{\min})/I_{\max} = 0.45$, and indicates partially polarized PL orienting along the *b*-axis of the belt. For comparison, the polarized PL signals excited by a laser with the polarization along the *c*-axis (width) of the CdSe belt have also been measured. As a result, the degrees of polarization are the same for both excitation polarizations along *b*- and *c*-axes.

The observed PL polarization in the CdSe nanobelts, however, differs from that of single CdSe nanorods reported to be along the rod axis (parallel to the *c*-axis, $||_c$) by Chen et al.[48] In contrast, the PL observed from single CdSe quantum dots by Empedocles et al.[49] shows that a pair of degenerate transition dipoles that locate in the *a*−*b* plane (perpendicular to the *c*-axis,

(45) Alivisatos, A. P.; Harris, T. D.; Brus, L. E.; Jayaraman, A. *J. Chem. Phys.* **1988**, *89*, 5979−5982.
(46) Tang, Z.; Kotov, N. A.; Giersig, M. *Science* **2002**, *297*, 237−240.
(47) Pankove, J. I. *Optical Processes in Semiconductors*; Prentice-Hall: New York, 1971; pp 8−12.
(48) Chen, X.; Nazzal, A.; Goorsky, D.; Xiao, M.; Adam peng, Z.; Peng, X. *Phys. Rev. B* **2001**, *64*, 245304.
(49) Empedocles, S. A.; Neuhauser, R.; Bawendi, M. G. *Nature (London)* **1999**, *399*, 126−130.

$\perp_c$) are responsible for the emission polarization of CdSe quantum dots. Depending on the shapes of CdSe nanocrystals, the distribution of electronic states of the nanocrystallite has been studied with a semiempirical pseudopotential calculation by Hu et al.[51] According to the calculation, PL from CdSe quantum dots or CdSe nanorods with an aspect ratio of <1.3 possesses $a-b$ planar ($\perp_c$) polarization, while the PL from nanorods elongating along the c-axis with an aspect ratio of >1.3 has linear ($||_c$) polarization.

Since the dimensions of as-synthesized CdSe nanobelts in this work are way beyond the exciton Bohr radius of CdSe (5−5.5 nm), the PL properties of CdSe nanobelts can, therefore, refer to those of bulk CdSe of wurtzite structure.[50,52] On the basis of the well studied selection rules for the allowed transitions in wurtzite semiconductors by Tronc et al.,[53] the PL of CdSe due to the zero-orbital-momentum excitons (s excitons) at the Γ point in the Brillouin zone (taking the spin−orbit coupling into account) can result from the recombinations of A exciton ($\Gamma_7^c \rightarrow \Gamma_9^v$, $\Delta E = E_g$) with $a-b$ planar ($\perp_c$) polarization, B exciton ($\Gamma_7^c \rightarrow \Gamma_7^v$, $\Delta E = E_g + 0.026$ eV)[54] with both $a-b$ planar ($\perp_c$) and c-axis linear ($||_c$) polarizations, and C exciton ($\Gamma_7^c \rightarrow \Gamma_7^v$, $\Delta E = E_g + 0.429$ eV)[54] also of $a-b$ planar ($\perp_c$) and c-axis linear ($||_c$) polarizations.

At room temperature in the present experiment, the two topmost valence bands of Γ_9^v and Γ_7^v, with a slight energy difference of 26 meV measured at 80 K[54] caused by spin−orbit coupling, can be populated with (excitonic) holes after laser excitation. The observed PL at ∼1.74 eV from the CdSe nanobelts (Figure 5) can be attributed to the recombinations of A exciton ($\Gamma_7^c \rightarrow \Gamma_9^v$) and B exciton ($\Gamma_7^c \rightarrow \Gamma_7^v$). In Figure 6a, the oscillation of PL intensity between 1 and 0.55 shows an angular dependence illustrating the contribution from different polarizations. The maximum PL intensity (normalized to 1) of the CdSe nanobelt at 0, 180, and 360° was measured with $\perp_c$ polarization, resulting from the recombinations of A exciton ($\Gamma_7^c \rightarrow \Gamma_9^v$) and B exciton ($\Gamma_7^c \rightarrow \Gamma_7^v$). Comparatively, the minimum PL intensity (relative intensity of 0.55) at 90 and 270° with $||_c$ polarization is due to the recombination of B exciton ($\Gamma_7^c \rightarrow \Gamma_7^v$) only. Accordingly, the PL polarization of CdSe nanobelts can approach a complete $\perp_c$ polarization (i.e., the degree of polarization ≈ 1) when the recombination of A exciton dominates the PL mechanism under a cryogenic condition at extremely low temperature.

(50) Efros, A. L. *Phys. Rev. B* **1992**, *46*, 7448−7458.
(51) Hu, J.; Wang, L.; Li, L.; Yang, W.; Alivisatos, A. P. *J. Phys. Chem. B* **2002**, *106*, 2447−2452.
(52) Thomas, D. G.; Hopfield, J. J. *Phys. Rev.* **1959**, *116*, 573−582.
(53) Tronc, P.; Smirnov, V. P. *Phys. Rev. B* **2002**, *66*, 165223.
(54) Lew Yan Voon, L. C.; Willatzen, M.; Cardona, M. *Phys. Rev. B* **1996**, *53*, 10703−10714.

Figure 6b shows two PL spectra of the CdSe nanobelt measured at the $\perp_c$ and $||_c$ emission angles, respectively, resulting from the recombinations of $\Gamma_7^c \rightarrow \Gamma_9^v + \Gamma_7^c \rightarrow \Gamma_7^v$ and $\Gamma_7^c \rightarrow \Gamma_7^v$. Separation between the peak maxima of the $||_c$ and $\perp_c$ bands is ∼22 meV, reasonably corresponding to the energy difference in the two topmost valence bands of Γ_9^v and Γ_7^v due to a spin−orbit splitting. This measured value is qualitatively in good agreement with the previously reported spin−orbit splitting of 26 meV for bulk CdSe of wurtzite structure measured at 80 K.[54]

Summary

High-quality hexagonal wurtzite CdSe nanostructures have been synthesized by a CVD method assisted with laser ablation. Wire-, belt-, and sheetlike CdSe structures have been obtained. Various morphological structures are fabricated at different thermal conditions. XRD results demonstrate that the as-grown CdSe nanobelts and sheets have a hexagonal wurtzite structure. Compared to that in bulk CdSe, lattice contraction in the CdSe nanostructures has been determined. ED and HRTEM images have shown that the single-crystalline hexagonal structures grew along the [0 1 −1 0] direction with side surfaces of ±(0 0 0 1) and top surfaces of ±(2 −1 −1 0). Phonon modes of CdSe nanobelts and bulk powder have been measured by SERS and NRS spectroscopies with off- and near-resonant excitations. Relative to bulk CdSe, the blue-shift of 2.4 cm^{-1} for the LO mode of CdSe nanobelts is caused by a lattice contraction in the belts. Room-temperature PL from the CdSe nanobelts exhibits a partially polarized dependence. Strong PL from a single CdSe nanobelt measured at room temperature promises a great potential for the application of CdSe nanobelts as optical and sensory devices.

Acknowledgment. Electron microscopic measurements in this study at Instrumentation Centers of National Taiwan University and National Tsing-Hua University, both sponsored by National Science Council of ROC, are acknowledged. This work is supported by CTCI Foundation and National Science Council of ROC (Grant Nos. 92-2113-M-002-039 and 92-2120-M-002-001).

Supporting Information Available: XRD spectra of CdSe nanobelts and bulk powder, an intermediate state of CdSe at ∼1.43 eV, laser power dependence of the SERS intensities of CdSe nanobelts. This material is available free of charge via the Internet at http://pubs.acs.org.

JA044270J